

**II-2.2. La Estructura en Profundidad. Artículo: “Crustal-scale structural architecture of the Central Chile Andes based on 3D seismic tomography, seismicity, and surface geology: Implications for mountain building in subduction zones”\***

**Crustal-scale structural architecture of the Central Chile Andes based on 3D seismic tomography, seismicity, and surface geology:**

**Implications for mountain building in subduction zones**

---

<b>Marcelo Farías*</b>	<i>Departamento de Geología, Universidad de Chile, Santiago, Chile LMTG, CNRS-IRD-Université de Toulouse, France Departamento de Geofísica, Universidad de Chile, Santiago, Chile</i>
Diana Comte	<i>Departamento de Geofísica, Universidad de Chile, Santiago, Chile</i>
Reynaldo Charrier	<i>Departamento de Geología, Universidad de Chile, Santiago, Chile</i>
Joseph Martinod	<i>LMTG, CNRS-IRD-Université de Toulouse, France</i>
Andrés Tassara	<i>Departamento de Geofísica, Universidad de Chile, Santiago, Chile</i>
Andrés Fock	<i>Departamento de Geología, Universidad de Chile, Santiago, Chile SQM S.A., Antofagasta, Chile</i>

---

**Keywords:** crustal seismicity; 3D seismic tomography; crustal-scale structural architecture; Central Chile Andes; subduction zone; mountain building

**\*Corresponding author:** [mfarias@dgf.uchile.cl](mailto:mfarias@dgf.uchile.cl).

Address: Plaza Ercilla #803, Casilla 13518 Correo 21, Santiago, Chile

---

---

\* Enviado el 4 de Septiembre de 2007 a *Earth and Planetary Science Letters*.

## Abstract

We document a crustal-scale structural model for the Central Chile Andes based on 3D seismic tomography, seismicity, and surface geology that consists of a major east-vergent ramp-flat structure connecting the subduction zone with the Andean Cordillera. The ramp rises from the subducting slab at  $\sim 60$  km depth to 15-20 km below the western edge of the cordillera, extending eastward below the high Andes as a 10 km-deep flat structure. The flat part of the structure defines a detachment that plays a fundamental role in the Andean orogenesis, because it accommodates most of the shortening in its hanging wall. This shortening is, however, very asymmetric:  $\sim 16$  km (1/5 of total) of the superficial shortening is accommodated in the western side of the cordillera, vs.  $\sim 80$  km (4/5 of total) in the eastern side of the belt. Yield strength envelopes suggest that the geometry of the structure at depth is controlled by the lithospheric rheology.  $V_p$  and  $V_p/V_s$  variations in the upper plate mantle (which may result from mantle serpentinization) and the deepest limit of the seismogenic interplate contact mark the intersection of the ramp with the slab. Then, the subduction factory process would control the depth where the major east-vergent structure merges to the slab. Such a ramp-flat structure seems to be a first-order characteristic of the Andean subduction zone, delimitating upward the rocks that transmit part of the plate convergence stress, transferring deformation from the plate interface, and controlling mountain building tectonics, thus playing a key role in the Andean orogeny as probably in other subduction orogens worldwide.

## 1. Introduction

The Andes is the Earth's largest and highest active mountain chain formed in a subduction margin. It is mainly the result of crustal shortening due to the convergence of the oceanic Nazca plate and the South American continent. Surface shortening has been mainly accommodated in backarc fold-and-thrust belts (**Fig. 1**) in the hanging wall of large east-vergent detachments (e.g., *McQuarrie [2002]; Cristallini and Ramos [2000]; Giambiagi and Ramos [2002]; Giambiagi et al. [2003]; Vergés et al. [2007]*). Therefore, detachments related to peripheral deformation belts appear to be the most significant structures controlling the Andean orogeny, as in several other modern and old orogens [*Cook and Varsek, 1994*]. However, the westward prolongation of detachments into the forearc region where plate interaction occurs is poorly understood, mainly because (1) surface deformation is much smaller in the western flank of the mountain belt, (2) most of the structures are west-vergent (e.g., *Muñoz and Charrier [1996]* for Northern Chile, and *Fock et al. [2006]* for Central Chile), and (3) there is no evidence for the downdip prolongation of these structures. This situation has led to a poor knowledge on the structural connection between the mountain belt and the subduction zone, as well as on the mechanism of stress and strain transfer from the interplate contact toward the orogen. Although some studies have attempted to balance the forces released in the subduction zone and those transferred to the orogen (e.g., *Isacks [1988]; Kono et al. [1989]; Lamb and Davis [2003]; Yáñez and Cembrano [2004]; Lamb [2006]*), these models have not considered the geometry of the structures involved in the resulting strain transfer.

For the Central Chile Andes (33-35°S), the construction of well constrained crustal-scale cross-sections, which is a pre-requisite for the study of orogenic processes, has presented several obstacles, such as difficulties to identify stratigraphic markers and to determine ages of

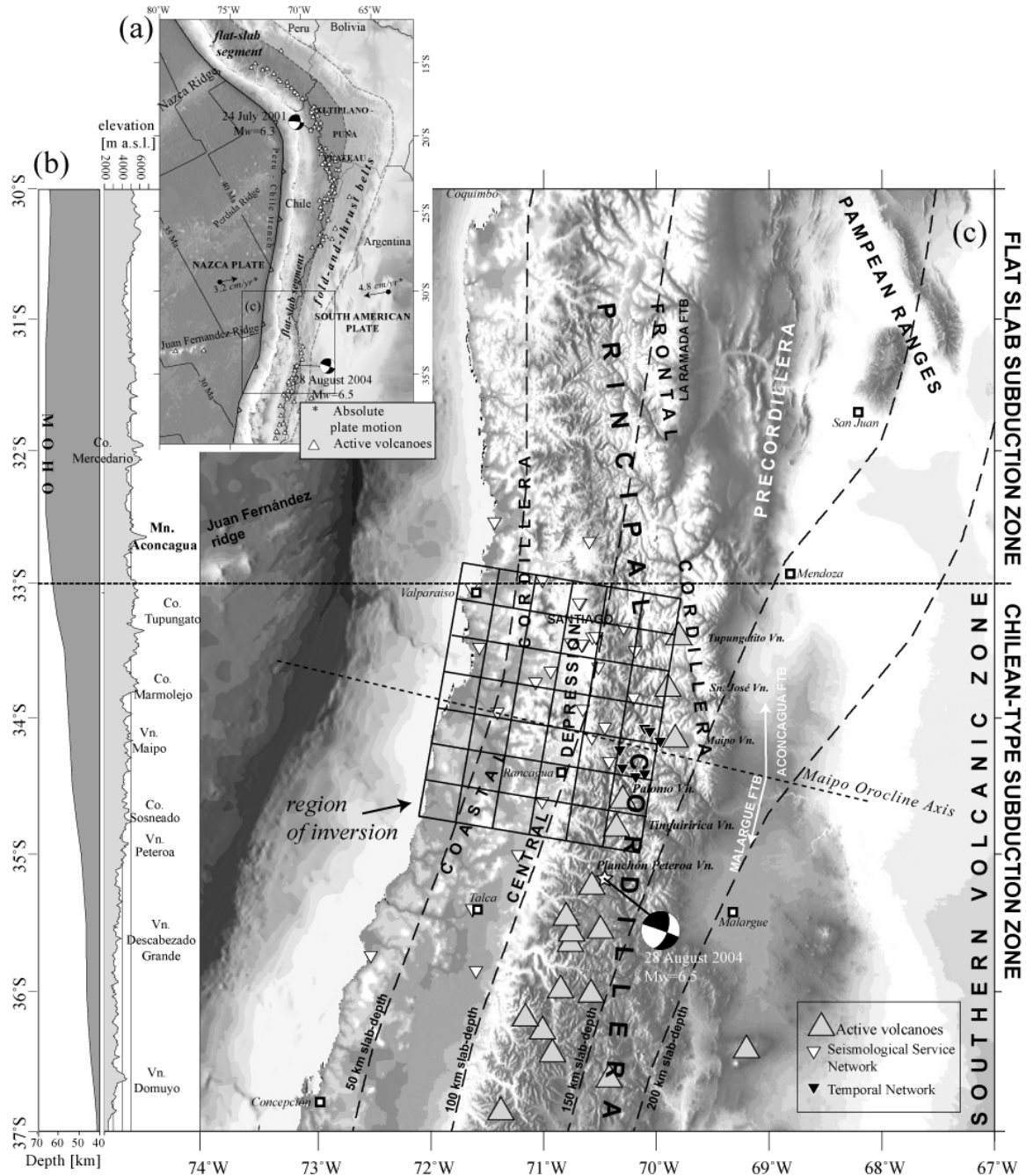


**Fig. 1.** (a) Tectonic framework of the Andean margin of Chile. (b) Maximum elevation and Moho depth from 32 to 37°S. Elevations calculated from SRTM90m DEM and crustal thickness after *Tassara et al.* [2006]. (c) Main tectonic and morphological features of the Andes of Central Chile and Western Argentina. Seismologic stations of the permanent network of the University of Chile (white inverted triangles) and temporary network deployed during January-April 2004 (dark inverted triangles) are shown. Grid in (c) corresponds to the region and cells in which tomography was performed. Absolute plate motion velocity after *Gripp and Gordon* [2002]. Focal mechanisms of the two greatest shallow crustal earthquakes of the last years are those estimated by Harvard CMT.

deposition and deformation because of the pervasive low-grade metamorphism affecting the rocks (e.g., *Levi et al.* [1989]; *Vergara et al.* [1993]), which are predominantly volcanic and plutonic units. However, the structural knowledge of the western side of the range has been improved in the last years by determining more accurate ages for the tectonic and depositional events due to a more systematic search for unaltered levels [*Fuentes, 2004; Muñoz et al., 2005*],

the application of more penetrative radioisotopic age determinations [*Charrier et al., 1996, 2002, 2005; Fock et al., 2006*], and the discovery of abundant localities containing a rich mammal fauna [*Wyss et al., 1990; Croft et al., 2003; Flynn et al., 1995, 2003*].

On the other hand, although most of the existing seismologic work in the Andes have paid attention to subduction zone processes related to the nucleation and propagation of megathrust earthquakes ( $M \geq 8$ ), the improvement of permanent seismologic networks and the deployment of temporary networks in the last years have allowed the detection of abundant crustal seismicity beneath the Chilean forearc-arc region. Two main events stand out in Chile (**Fig. 1**): the 24 July 2001 ( $M_w=6.3$ ) Aroma earthquake in the western flank of the Altiplano at 19°30'S [*Farías et al., 2005; Legrand et al., 2007*], and the 28 August 2004 event ( $M_w=6.5$ ) in the High Andes at 35°15'S [*Farías et al., 2006*]. Crustal seismicity occurring in main fault systems emphasizes its relevance for understanding the significance of these structures in mountain building, their subsurface prolongation into the continental lithosphere, and their association with main detachments and links to the subduction interface.

In this contribution, we integrate seismologic and geological data from the Central Chile Andes (33-35°S) to address two main questions: (1) how is the forearc-arc structural array connecting the subduction zone to the fold-and-thrust belts located in the backarc, and (2) what has been the contribution of this general structure in the construction of the Andes of Central Chile. This study is based on the analysis of seismicity recorded by both the permanent network of the Seismologic Survey at the Universidad de Chile (SS) and a temporary network deployed along one of the largest structural systems in the high Andes of Central Chile [*Barrientos et al., 2004; Charrier et al., 2005*]. We correlate these data with surface geology in order to infer the crustal-scale structural architecture of the entire mountain range (forearc, arc, and backarc). We suggest that a major detachment runs below the entire mountain belt and that this structure is connected to the subduction zone through a ramp that cuts across the forearc lithospheric wedge. We finally propose a qualitative approach to the mechanisms controlling the deformation transfer from the interplate interface toward the mountain belt, which could be significant for understanding orogenic mechanisms not only in the study region, but also in the entire Chilean subduction margin and in other subduction orogens.

## 2. Tectonic and geological settings

The subduction of the oceanic Nazca plate beneath the South American continent is the most important tectonic process along the Andean margin. Current absolute plate motion relative to hotspots frame [*Gripp and Gordon, 2002*] for the South American and Nazca plates are 4.8 and 3.2 cm/yr, respectively (N78°E, ~ 8 cm/yr relative plate motion; **Fig. 1a**).

The Chilean-Pampean flat-slab subduction region (27°S-33°S), where slab dip is <10° between 100 and 150 km depth, represents a major along-strike change on the Andean subduction system. North and south of this segment, the dip of the slab is greater (~ 30°E) being the classic example for the “Chilean-type Subduction” [*Uyeda and Kanamori, 1979*]. This segmentation has been interpreted as the result of buoyancy force exerted by the subduction of the Juan Fernández ridge at 32.5°S (**Fig. 1**) [*Pilger, 1981; Nur and Ben-Avraham, 1981; Gutscher et al., 2000;*

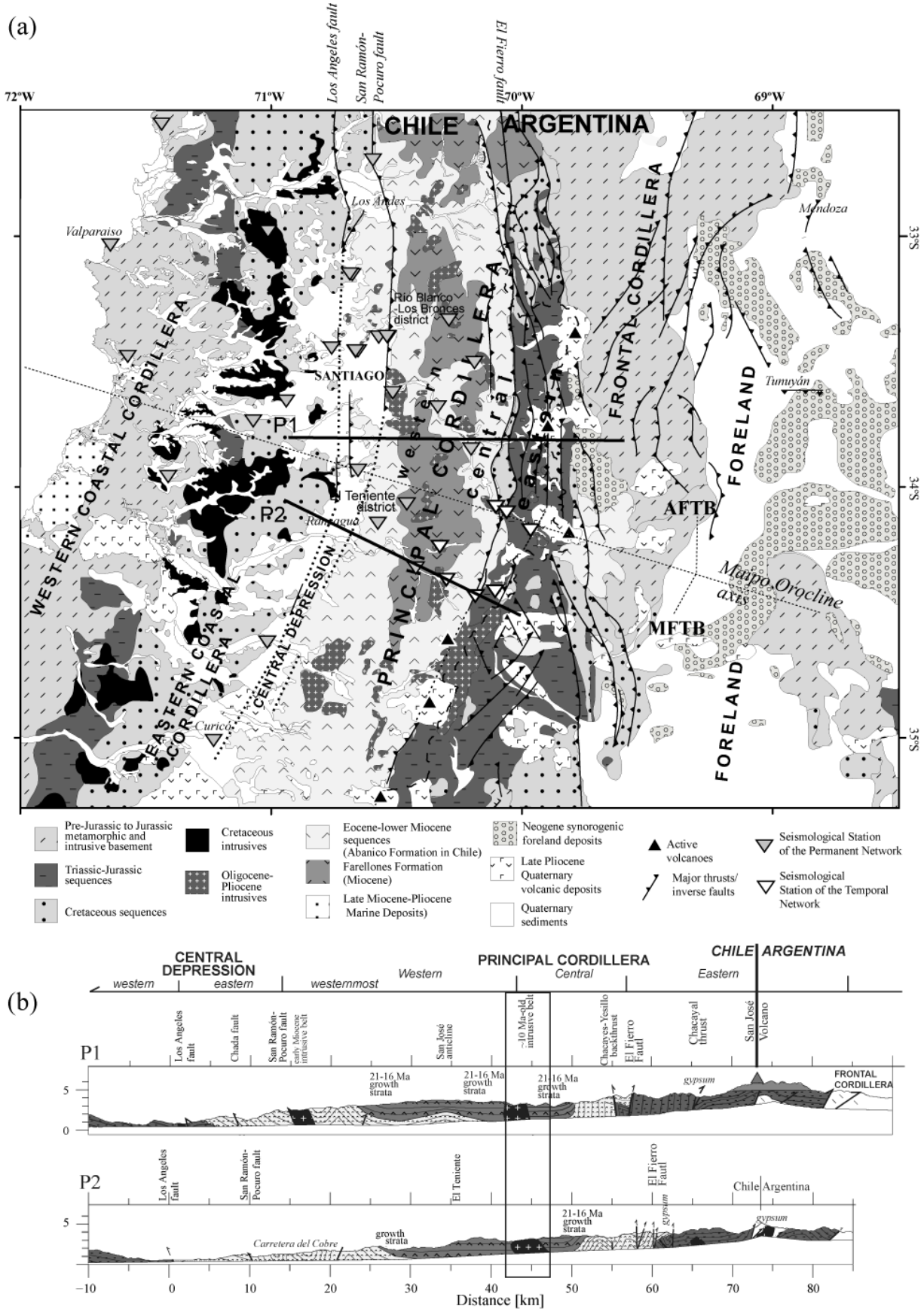


**Fig. 2.** Simplified geological map (a) and cross-sections (b) of the Andes of Central Chile and Argentina. Only main inverse faults active during the Neogene are plotted. Modified after *SEGEMAR [1997]*, *Godoy et al. [1999]*, *Charrier et al. [2002]*, *SERNAGEOMIN [2002]*, *Giambiagi et al. [2003]*, and *Fock et al. [2006]*.

*Yáñez et al. 2001*]. In addition, some distinctive features appear approximately at 33°S (Fig. 1b,

c), namely, a change in the strike of both the trench and the mountain belt from N-S northward to NNE-SSW southward (Maipo Orocline), the absence of volcanism since *ca.* 9 Ma above the flat-slab region [Kay *et al.*, 1991], the decrease in elevation and in crustal thickness south of 33°S [Tassara *et al.* 2006], the increase in flexural rigidity south of 34°S in the arc (e.g., Pérez-Gussinyé *et al.* [2007]; Tassara *et al.* [2007]), the southward segmentation of the mountain range by a longitudinal valley (Central Depression), and the southern edge of the Frontal Cordillera, Pampean Ranges and Precordillera.

The Andean region between 33°S and 35°S comprises five main morphostructural units (Fig. 1 and 2), which are, from west to east, the Coastal Cordillera, the Central Depression, the Principal Cordillera (subdivided into a western, central and eastern Principal Cordillera), the Frontal Cordillera (not present south of 34°15'S), and the active foreland region. The Coastal Cordillera consists of a late Paleozoic-Triassic basement in its western flank and east-dipping Jurassic to Cretaceous sequences extend in its eastern flank and in the western Central Depression (Thomas [1958]; see Fig. 2). From the eastern half of the Central Depression to the central Principal Cordillera, an extensional basin developed during Eocene to late Oligocene times (Abanico basin), which began to be inverted in the early Miocene [Godoy *et al.*, 1999; Charrier *et al.*, 2002]. This basin was filled by the predominantly volcanic-volcanoclastic Abanico Formation. In the early stages of inversion, folding and high-angle reverse faulting were concentrated at both basin edges [Fock *et al.*, 2006]. In the center of the basin, the mainly volcanic Farellones Formation was deposited during early to middle Miocene times. This unit is generally mildly folded, excepting at its contacts with the Abanico Formation where it is either overlying unconformably the Abanico Formation or developing growth strata in its lower layers (older than 16 Ma) [Charrier *et al.*, 2002, 2005; Fock *et al.*, 2006]. After ~ 16 Ma, contractional deformation migrated toward the eastern Principal Cordillera. There, Mesozoic sequences (mainly sedimentary rocks deposited into a rift-related backarc basin) have accommodated most of the shortening in this region [Giambiagi and Ramos, 2002; Giambiagi *et al.*, 2003]. After 8.5 Ma and further east, the late Paleozoic granitoids of the Frontal Cordillera were uplifted by the activity of high-angle inverted normal faults rooted in the basement. Simultaneously or shortly after, high-angle out-of-sequence reverse faults affected the eastern bounding fault system of the Abanico basin and the eastern Principal Cordillera [Giambiagi and Ramos, 2002; Giambiagi *et al.*, 2003; Fock *et al.*, 2006]. At ~ 4 Ma, shortening migrated further east to the foreland [Giambiagi *et al.*, 2003].

### 3. Structural features of the mountain belt in Central Chile and Western Argentina

We present two structural cross-sections (Fig. 2b) in which we integrate structural information reported by previous authors (e.g., Thiele [1980], Giambiagi *et al.* [2003], Fock *et al.* [2006], for the Santiago cross-section; P1 in Fig. 2b; Charrier [1981], Godoy *et al.* [1999], and Charrier *et al.* [2002, 2005] for the Cachapoal cross-section; P2 in Fig. 2b) with new data obtained during the field work performed for this study.

### 3.1. Eastern Central Depression and western Principal Cordillera

Only Cenozoic deposits crop out in this sector (Abanico and Farellones formations, and intrusive bodies). The western edge of this region is characterized by east-dipping partially inverted normal-faults (Los Angeles fault system according to *Carter and Aguirre* [1965], Infiernillo fault according to *Fock et al.* [2006]; Fig. 2) in which the Cenozoic units override Mesozoic sequences. This fault system is the western edge of the Abanico Basin [*Fock et al.*, 2006]. The western edge of the Principal Cordillera is defined by a west-vergent reverse fault system (San Ramón-Pocuro fault and its southward prolongation (*Thiele* [1980]; *Charrier et al.* [2005]; *Fock et al.* [2006]; *Rauld et al.* [2006]; Fig. 2). Based on geomorphologic markers, this structure would have accommodated 0.7-1.1 km of relative surface uplift of the eastern hanging wall since the late Miocene at the latitude of Santiago, and 800-600 m at 35°S [*Fariás et al.*, 2007]. Immediately east of this edge, a series of synclines and anticlines developed prior to ~ 16 Ma, which is evidenced by growth strata in the lower layers of the Farellones Formation [*Fock et al.*, 2006] (Fig. 2b). To the east, some folds and faults deform subtly the Cenozoic sequences with a predominant east-vergency (Fig. 2b).

### 3.2. Central Principal Cordillera

Only Cenozoic deposits also crop out in this sector. These units are bounded to the east by east-vergent faults, along which the Abanico Formation overrides the Mesozoic sequence situated in the eastern Principal Cordillera. These faults constitute the eastern boundary of the Abanico basin. This fault system extends more than 300 km along-strike (Fig. 2a). The main faults of this system received different names according to their latitude: El Diablo fault at 33°45'S [*Fock et al.*, 2006], Las Leñas-Espinoza fault at 34°30'S [*Charrier et al.*, 2002], and El Fierro fault at approximately 35°S [*Davidson and Vicente*, 1973] (hereafter, we name this system El Fierro fault). In the eastern flank of the central Principal Cordillera, both east- and west-vergent folds and thrusts affect the Abanico Formation. The folds exhibit maximum amplitudes of 3 km and are normally cut by faults that were reactivated during the out-of-sequence thrusting event (late Miocene-early Pliocene). Among them, the west-vergent Chacayes-Yesillo fault (see profile P1 in Fig. 2b) stands out because of its >2 km of vertical throw [*Charrier et al.*, 2005].

### 3.3. Eastern Principal Cordillera and Frontal Cordillera

The eastern Principal Cordillera extends east of the El Fierro fault and consists of Mesozoic marine and continental sedimentary deposits that include an Oxfordian gypsum level (Fig. 2b) and minor volcanic layers. These deposits are overlain by Neogene syntectonic foreland-basin deposits that evidence the beginning of deformation shortly after 16 Ma [*Giambiagi et al.*, 2003]. Most of the shortening in this region (~ 47 km) has been accommodated by east-vergent thrusts and related backthrusts [*Giambiagi and Ramos*, 2002], which commonly take advantage of the gypsum levels (Fig. 2b). The structural restoration of *Giambiagi and Ramos* [2002] suggests that these thrusts root in a ~ 10 km depth east-vergent detachment fault.

North of  $34^{\circ}15'S$ , the crystalline basement of the Frontal Cordillera crops out east of the Principal Cordillera. There, several basement blocks have been uplifted by high-angle east-vergent inverse faults accommodating about 15 km of shortening between 9 and 6 Ma. *Giambiagi et al.* [2003] interpreted this thick-skinned style as a result of the inversion of normal faults related to the Mesozoic backarc rifting. According to these authors, the reactivation of these structures would require a detachment fault located at mid-crustal levels.

#### 4. Seismologic data and procedure

We used the seismologic data recorded by the Seismologic Survey at the Universidad de Chile (SS) between 1980 and 2004. This record is complemented with a temporary network deployed from January to April 2004 (**Fig. 1 and 2**). The SS has 24 seismologic stations in the study region and the temporary network consisted of 7 short period 3-component stations. The final database includes 23444 events, with 212 shallow (<20 km depth) crustal events recorded by the temporary network.

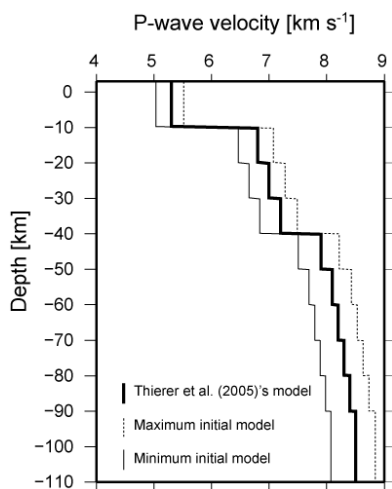


**Fig. 3.** Initial 1D P-wave velocity models.

The hypocenters were first estimated using the HYPOINVERSE program [*Klein, 1978*] with a 1D  $P$ -wave velocity model based on *Thierer et al.* [2005] (**Fig. 3**). Each earthquake was located with different trial depths in order to minimize the effect of the initial conditions on the final hypocentral determination. Trial depths were varied between 0 and 250 km with an increment of 5 km. The location with the lowest root mean square misfit and with the maximum number of body-waves first-arrivals was selected for each event. This procedure ended with  $\sim 140000$  and  $\sim 95000$   $P$ - and  $S$ -arrival times, respectively.

From the preliminary hypocenters and seismic wave arrival times, a 3D velocity structure was calculated using the SPHYFIT90/SPHREL3D90 program (see details in *Roecker et al.* [1993]). Inversion was made on a region divided into  $6 \times 7$  blocks with a grid spacing of  $30 \times 30 \text{ km}^2$  (see **Fig. 1**) and 12 layers of 10 km thick, except the shallowest one, which is 13 km thick. Because  $P$ -wave and  $S$ -wave velocities were inverted independently, this procedure ended with 1008 final blocks with 877 blocks considered as reliable (those having  $>20$  rays hits, however most of block are hit by  $>1000$  rays). The resulting velocity models were used to relocate the hypocenters, which were classified and filtered according to the same criteria used by *Abers and Roecker* [1991]. Filtered hypocenters were used for a new inversion. This procedure was repeated iteratively until the changes in velocities became very small ( $<1\%$ ), being three iterations required. In order to test the resulting tomography, 6 different models were made with initial 1D velocity structures perturbed  $\sim 5\%$  randomly from the *Thierer et al.* [2005] model (**Fig. 3**). The resulting models had a standard deviation  $<3\%$ , thus we considered the mean velocity of them as the final  $V_p$  and  $V_s$  models.

From the preliminary 23444 events, only 18259 passed filtering, which were filtered again in order to use only the most reliable data. For the events recorded only by the SS, the criterion of selection was defined by  $P$ - plus  $S$ -wave phases  $\geq 10$ , RMS residual  $\leq 0.3$  s, and standard errors in position  $\leq 1.5$  km, resulting in 9065 events. For the hypocenters recorded by the temporary network, the criterion of selection consisted of RMS residual  $\leq 0.3$  s and  $P$ - plus  $S$ -wave phases  $\geq 9$ , remaining only 92 hypocenters.

## 5. Results and Analysis of Seismologic Data

### 5.1. General results

The final distribution of hypocenters shows that most of the crustal seismicity is located beneath the Principal Cordillera and eastern Central Depression at depths shallower than 20 km (**Fig. 4**). Superficial seismicity in the offshore and coastal forearc mainly corresponds to events occurring in the interplate contact area, except some earthquakes located in the overriding plate. As previously suggested by *Barrientos et al. [2004]* and *Charrier et al. [2005]*, most of the shallow crustal seismicity is located close to the Chile-Argentina boundary and is aligned with the El Fierro fault (**Fig. 4**).

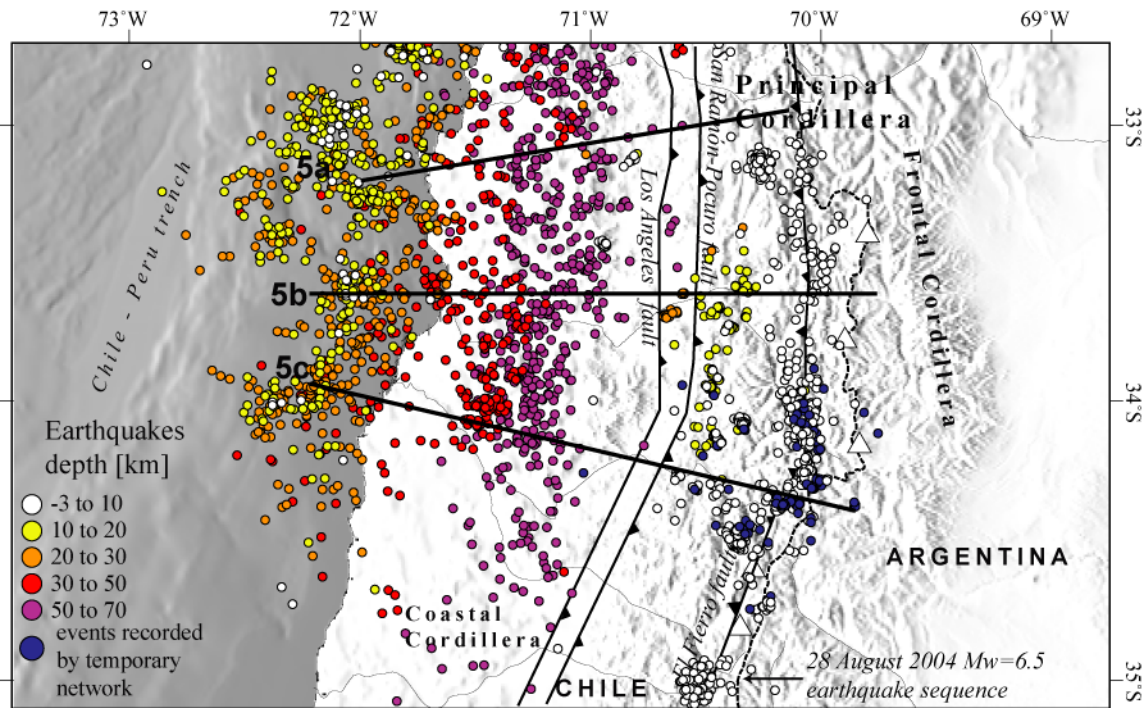


**Fig. 4.** Regional distribution of final relocated epicenters. Solid lines correspond to the locations of cross-sections in Fig. 5.

## 5.2. Ramp-flat seismic structure

In order to analyze the relationship between seismicity, seismic velocity fields and lithospheric structure, we show in **Fig. 5** three profiles crossing perpendicularly the orogen-strike and covering most of the study region. At first sight, the geometry displayed by seismicity can be interpreted as a ramp-flat crustal-scale structure.

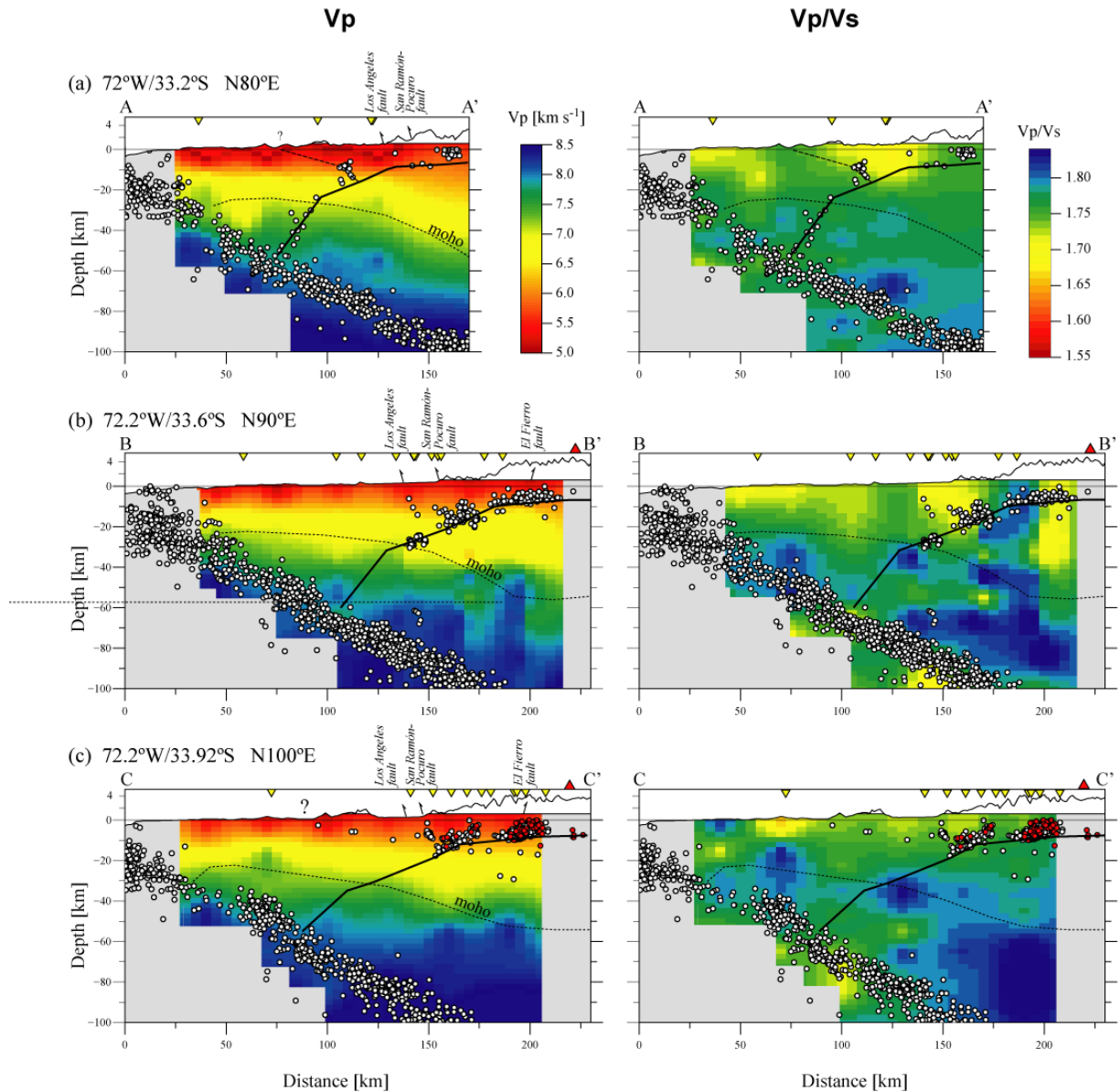


**Fig. 5.** Crustal-scale cross-sections perpendicular to the orogen-strike showing velocity structures and relocated hypocenters obtained in this work. Location and orientation of sections are indicated in Fig. 4. Moho depth after *Tassara et al.* [2006]. In all sections, earthquakes were projected onto the cross-section from a box-width of 40 km (-20 km/+20 km) centered along the swaths. White circles are the events recorded by the permanent seismicologic network, whereas the red circles are those obtained from the temporary network.

Seismicity associated with the flat geometry is located beneath the Chilean Principal Cordillera. This structure dips  $\sim 10^\circ\text{W}$  in the western Principal Cordillera, where it is located at 15-10 km depth. In the central-eastern Principal Cordillera, the structure is located at 10-5 km depth and dips  $<5^\circ\text{W}$ . In this sector, the flat-structure coincides fairly well with the geometry and depth proposed by *Giambiagi et al.* [2003] for the detachment that has controlled the thin-skinned deformation in the eastern Principal Cordillera.

The ramp segment dips  $\sim 40^\circ\text{W}$  and extends downward from the western edge of the Principal Cordillera to the Moho below the Central Depression. Although seismicity in the ramp segment is absent in southern sections (possibly reflecting the aseismic behavior of the lithospheric mantle), it is well detected in the section across the Central Depression at  $33.2^\circ\text{S}$  (**Fig. 5a**). In this section, the ramp intersects the Wadatti-Benioff zone at  $\sim 60$  km depth.

The ramp can be correlated with discontinuities on  $V_p$  and  $V_p/V_s$  within the lithospheric mantle wedge (**Fig. 5**). Discontinuity on P-wave field consists in a sharp eastward velocity increase from 7.3-7.7 to 7.9-8.2 km/s. Discontinuities on  $V_p/V_s$  are less evident; however, the ramp can be correlated with normal  $V_p/V_s$  ( $\sim 1.75$ ), whereas high  $V_p/V_s$  ( $>1.80$ ) are located in the surrounding zones (**Fig. 5**).

Because these features are observed everywhere in the study region, they can be considered as a main characteristic of the forearc in Central Chile. Therefore, the downward prolongation of the ramp into the mantle should be determined by the existence of rheological discontinuities within the lithosphere near the plate interface.

## 6. Yield Strength Envelope analysis

The strength of the continental lithosphere is controlled by its depth-dependent rheological structure, which in turn depends on the thickness and composition of crustal layers, the thickness of the lithospheric mantle, the temperature structure, the strain rate, and the presence or absence of fluids (e.g., *Carter and Tsenn* [1987]; *Kirby and Kronenberg* [1987]; *Burov and Diament* [1995, 1996]; *Cloetingh et al.* [2005]).

In order to analyze the rheological control on the ramp-flat structure, we constructed four 1D columns of compressional yield strength envelopes (**Fig. 6**). They are based on the 3D lithospheric compositional and geometrical model of *Tassara et al.* [2006] (**Fig. 6a**), a 2D geothermal gradient based on *Oleskevich et al.* [1999] and *Yáñez and Cembrano* [2004] (**Fig. 6b**), and experimental rheological parameters for quartzite (upper-crust), dry-diabase (lower-crust) and wet-dunite (lithospheric mantle) [*Carter and Tsenn*, 1987; *Burov and Diament*, 1995].

Resulting yield strength envelopes (**Fig. 6c**) illustrate that in the western flank of the eastern Principal Cordillera (Column IV), low-viscosity ductile rocks should prevail both between 8 and 20 km depth (upper crust) and between 35 and 60 km depth (lower crust). These low-viscosity ductile zones are confined by three “rigid” (high-strength brittle and/or high-viscosity ductile) layers located between 12 and 3 km depth, between 20 and 35 km depth, and

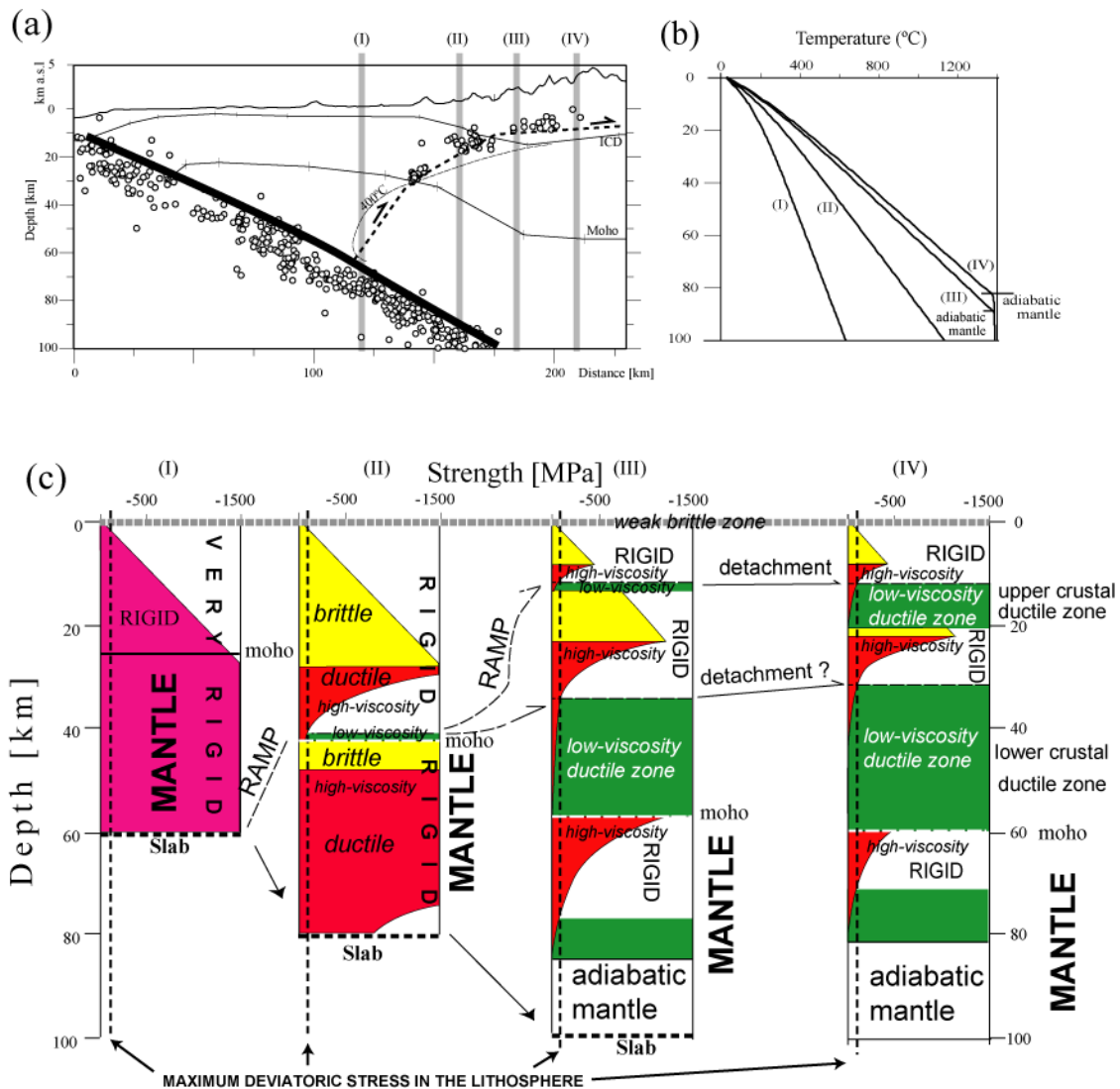


**Fig. 6.** Compressional yield strength envelopes analysis. (a) Figure 5b used as reference to indicate the location of the columns where yield strength envelopes were calculated. Moho and IntraCrustal density discontinuity (ICD) depth after *Tassara et al. [2006]*. The 400°C isotherm is reported for reference. (b) Geothermal gradient for the four columns used for yield strength envelop calculation. (c) Resulting Yield strength envelopes. Geothermal gradient approximated from *Oleskevich et al. [1999]* and *Yáñez and Cembrano [2004]*. The ICD delimitates an upper crust with quartzite composition ( $H=1.9 \times 10^5$  [J mol<sup>-1</sup>],  $A=5 \times 10^{-12}$  [N<sup>-3</sup>m<sup>6</sup>s<sup>-1</sup>] [*Burov and Diament, 1995*]) from a lower crust with quartz-diorite composition ( $H=2.12 \times 10^5$  [J mol<sup>-1</sup>],  $A=5.1 \times 10^{-15}$  [N<sup>-2.4</sup>m<sup>5.76</sup>s<sup>-1</sup>] [*Burov and Diament, 1995*]). Mantle has been considered with a wet dunite composition ( $H=4.44 \times 10^5$  [J mol<sup>-1</sup>],  $A=7.94 \times 10^{-17}$  [N<sup>-3.35</sup>m<sup>11.22</sup>s<sup>-1</sup>] [*Carter and Tsenn, 1987*]). Maximum deviatoric compressive stress in the continental lithosphere ( $\sim 100$  MPa) according to *England and Molnar [1991]*. Location of columns: (I) is below the Central Depression, (II) is below the western edge of the Principal Cordillera, (III) is below the central Principal Cordillera and (IV) is beneath the Chilean side of the eastern Principal Cordillera.

immediately below the Moho. The geothermal gradient diminishes to the west. Column III (western edge of the central Principal Cordillera) shows that the upper low-viscosity ductile zone wedges out toward the west and disappears beneath the western Principal Cordillera (Column II). This analysis predicts a coupled upper and lower crusts beneath the westernmost Principal Cordillera and Central Depression (Column I). Yield strength envelopes also suggest that the viscosity in the base of the crust would remain small beneath the western edge of the Principal

Cordillera, but further west the crust and the upper mantle would be strongly coupled (Column I). Therefore, the lithospheric forearc west of the Central Depression would be very rigid.

Beneath the Principal Cordillera (columns III and IV), the top of the upper crustal low-viscosity ductile zone is fairly well correlated with the flat segment of the seismic structure (**Fig. 6c**). The western edge of the flat segment correlates well with the western edge of this low-viscosity ductile zone (columns II and III). The ramp segment extends from there downward to the top of the lower crustal low-viscosity ductile zone near the Moho (Column II). This “shift” from an upper to a lower detachment level is coherent with ramp structures, which generally connect weak zones across a more rigid layer (see *Cook and Varsek [1994]*, and references therein). In spite of the lack of direct evidence for the lower ductile zone, the activity of its top as a deep detachment could explain the reactivation of the deep basement structures that controlled the uplift of the Frontal Cordillera in the late Miocene (c.f., *Giambiagi and Ramos [2002]*; *Giambiagi et al. [2003]*).

Yield strength envelopes predict that the rocks located above the detachment beneath the Principal Cordillera should prevail very rigid. However, this zone concentrates abundant seismicity that is normally aligned with some structures observed at the surface. Because this zone has been widely deformed during the Neogene (**Fig. 2b**), it is likely that seismicity in this region is related to the reactivation of older discontinuities and fractures. Indeed, *Charrier et al. [2002, 2005]* proposed that the deformation within the Abanico Formation is mostly related to the inversion of the normal fault that controlled the development of the extensional basin during Eocene-Oligocene times. Likewise, Neogene deformation in the eastern Principal Cordillera and Frontal Cordillera is related to the reactivation of older normal faults as well as faulting along less competent rocks such as gypsum levels [*Giambiagi and Ramos, 2002*; *Giambiagi et al., 2003*]. Therefore, seismicity above the detachment would be related to the reactivation of older structures and discontinuities rather than new formed faults.

## 7. Integrating seismologic data and surface geology

At depth, the flat structure visualized by seismicity coincides fairly well with the detachment proposed by *Giambiagi and Ramos [2002]* and *Giambiagi et al. [2003]*. In order to analyze the role of this structure on mountain building, we constructed two upper-crustal cross-sections integrating both surface geology and seismicity (**Fig. 7**). These sections display the structure only in the Chilean side of the cordillera: the Argentinean side of the belt has been already studied in detail by *Giambiagi and Ramos [2002]* and *Giambiagi et al. [2003]*. Cross-sections are constrained by down-plug projection of surface structure and its correlation with seismicity, geometrical constraints, and the age of deformation. Despite the precise downward prolongation of some particular faults may be debated, these cross-sections give the general geometry of the major orogen-scale structures, constrained using both surface geology and seismicity.

In the zone where the Abanico basin developed (eastern Coastal Cordillera, western and central Principal Cordillera), the orogen approximately displays a symmetric double-vergency system of faults, preserving a central portion that remains almost non-deformed (**Fig. 7**). A

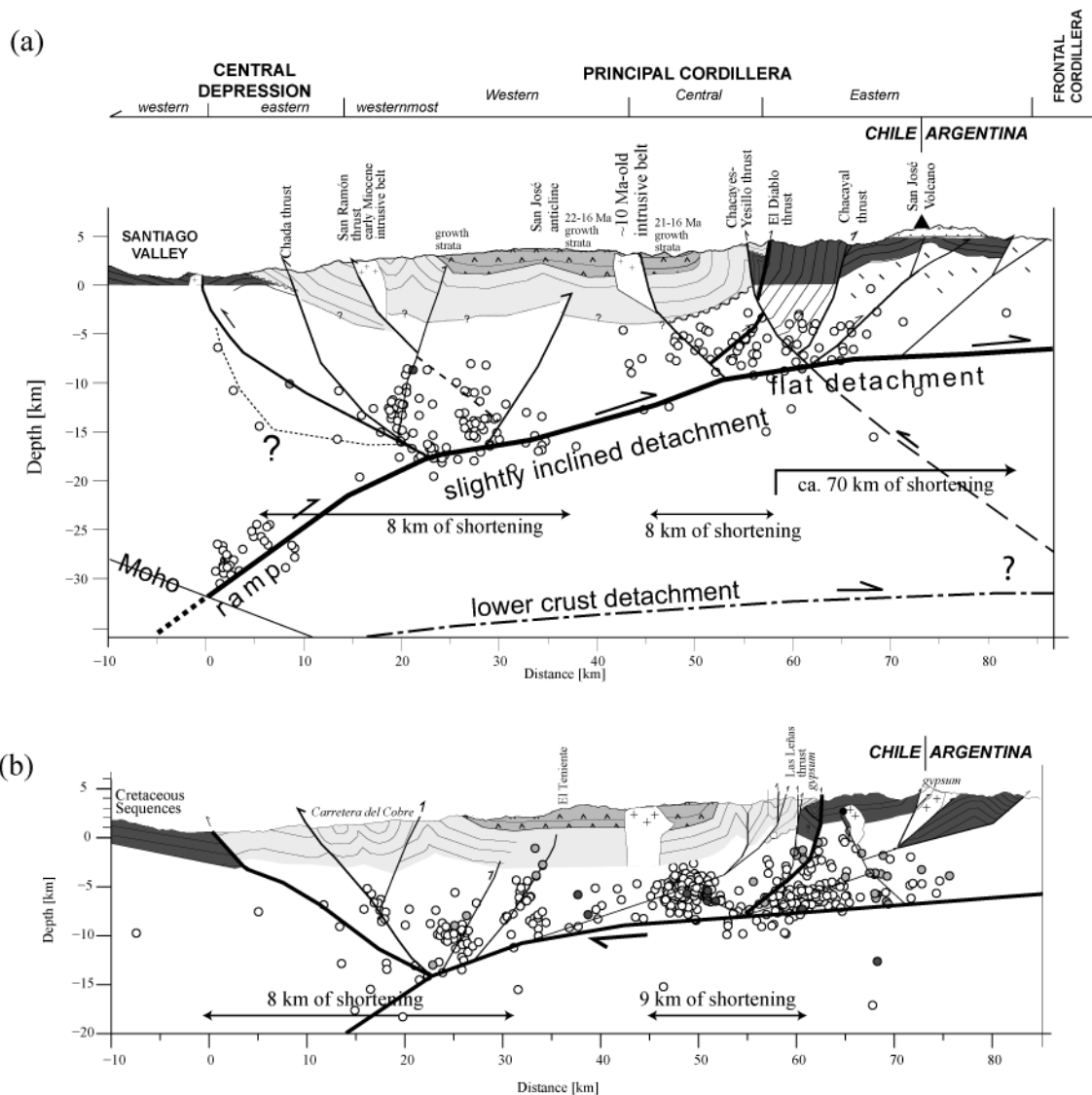


**Fig. 7.** Structural cross-section and shallow seismicity. (a) Maipo profile (P1 in Fig. 2b) (b) Cachapoal profile (P2 in Fig. 2b). Structural restoration shows that about 16 km of shortening has been accommodated in the segment where the Abanico and Farellones formations crops out. This shortening is distributed almost equitably on both flanks of the former extensional basin.

minimum estimation of shortening in this part of the chain is 16 km ( $\sim 20\%$  of the total shortening across the mountain belt, see **Table 1**). At this place, most of the contractional deformation occurred in the lower Miocene, resulting in the inversion of the Abanico basin. Deformation is distributed almost equitably on both flanks, thus, the resulting geometry is consistent with the inversion of an extensional ramp-flat listric fault system [*McClay, 1995*] (**Fig. 7**). During the basin inversion, the eastern Principal Cordillera accommodated  $\sim 6$  km of shortening [*Giambiagi and Ramos, 2002*].

After 16 Ma, shortening ended within Abanico basin migrating eastward. Deformation began in the eastern Principal Cordillera, propagating into the Frontal Cordillera, returning into the eastern Principal Cordillera, and finally migrating to the foreland [*Giambiagi et al, 2003*]. Deformation in the eastern side of the cordillera has been predominantly accommodated by east-

vergent thrusts and related backthrust. Shortening in the eastern Principal Cordillera, Frontal Cordillera, and foreland is ~ 62 km [*Giambiagi and Ramos, 2002*], which represents about 80% of the total shortening across the chain at approximately 33.8°S (see **Table 1**).

In the structural model presented in this work (**Fig. 7**), some faults in the central and eastern Principal Cordillera are not consistent with the eastward tectonic transport of the upper crustal detachment. This is the case of the west-vergent Chacayes-Yesillos fault (**Fig. 7a**), which must be connected to a deeper detachment, likely corresponding to the lower crustal detachment predicted by the yield strength envelopes analysis. Because the Chacayes-Yesillos fault was active during the out-of-sequence thrusting event between 8.5 and 4 Ma [*Fock et al., 2006*], it would be related to the reactivation of the high-angle faults that controlled the block-like uplift of the crystalline basement that forms the Frontal Cordillera [*Giambiagi et al., 2003*].

Considering the timing of deformation, most of the shortening occurs during three major events at 33.8°S (**Table 1**). (1) Abanico basin inversion (~ 16 km of shortening between 22 and 16 Ma, and 6 km of shortening in the eastern Principal Cordillera before 15 Ma), (2) thin-skinned fold-and-thrust belt development in the eastern Principal Cordillera (24 km of shortening between 16 and 8.5 Ma [*Giambiagi and Ramos, 2002*]), and (3) uplift of the Frontal Cordillera (15 km of shortening between 8.5 and 6 Ma) and out-of-sequence thrusting in the central-eastern Principal Cordillera (17 km of shortening between 8.5 and 4 Ma [*Giambiagi and Ramos, 2002*]). The out-of-sequence thrusting event in the eastern Principal Cordillera represents a disruption of the eastward migration of shortening. Shortening migrated eastward along the detachment until the high-angle basement faults rooted in the Frontal Cordillera were reactivated. This reactivation caused the return of the deformation to the axis of the mountain belt as out-of-sequence thrusting (c.f., *Cristallini and Ramos [2000]; Giambiagi et al. [2003]*).

After 4 Ma, shortening migrated to the foreland, accommodating about 6 km of shortening [*Giambiagi and Ramos, 2002*]. In turn, the high Cordillera has not accommodated shortening since that time, but strike-slip deformation is presently reported by seismicity [*Farías et al., 2006*].

**Table 1.** Shortening\* across the Andes at 33.8°S

	First stage 22-15 Ma	Second Stage 15-8.5 Ma	Third Stage 8.5-4 Ma	Four Stage 4-0 Ma	Total
Abanico basin	16 <sup>§</sup>				16
Eastern Ppal. Cord.	6	24	17		47
Frontal Cordillera			15		15
Foreland				6	6
<b>Total</b>	<b>22</b>	<b>24</b>	<b>32</b>	<b>6</b>	<b>84</b>

\* Approximated shortening [km]  
<sup>§</sup> Estimated in this work. The remaining values according to *Giambiagi and Ramos [2002]*

## 8. Implications for mountain building in subduction zones

Before 22 Ma, the crustal thickness was moderate (<35 km thick), being approximately uniform beneath both western and eastern flanks of the Abanico basin as suggested by studies on the geochemistry of the basin-related volcanic rocks (e.g., *Fuentes [2004]; Kay et al. [2005]; Muñoz et al. [2006]*). Although both flanks of the Abanico basin had similar initial crustal thickness before inversion and have accommodated a similar amount of shortening, the present-day crust is ~ 20 km thicker below the eastern boundary of the basin (central Principal Cordillera) (**Fig. 8**). This suggests that some of the 4/5 of the total surface shortening of the chain accommodated east of the Abanico basin by east-vergent thrust-systems has been transferred to the west beneath the detachment as a “simple shear mode” (in the sense of *Allmendinger and Gubbels [1996]*). The importance of deep shortening in the western part of the chain is also supported by the fact that most of the surface and rock uplift of the western and central Principal Cordillera occurred between 10 and 4 Ma, even though most of the surface shortening was accommodated before 16 Ma [*Fariás et al., 2007*]. Likewise, the advance to west of the crust beneath the detachment would be opposed by the increasing rigidity of the lithosphere in the forearc (**Fig. 6**). This opposition seems to be evidenced by the seismic cluster located in the ramp immediately above the Moho (**Fig. 8**).

A major east-vergency ramp-flat structure, whose geometry is also controlled by the rheology of the continental plate, has been already proposed for the Northern Chile margin by *Fariás et al. [2005]* and *Tassara [2005]* based on the works of *Isacks [1988]* and *Lamb et al. [1997]*, among others. These authors proposed that this structure would be connected to the detachment fault that prolongs through the Altiplano to the Eastern Cordillera and Subandean zone where most of the shortening has been accommodated [e.g., *McQuarrie, 2002*]. To the west, the ramp encloses upward a rigid forearc acting as a pseudo-indenter that resists the westward advance of the crustal mass located beneath the detachment. It results in crustal thickening in the Precordillera and Western Cordillera, in a zone where the surface shortening has been moderate and essentially older than uplift [e.g., *García, 2002; Victor et al., 2004; Fariás et al., 2005; Hock et al., 2007; Riquelme et al., 2007*].

The east-vergent ramp emerging from the interplate contact area has been visualized at different latitudes along the margin, intersecting the slab approximately at the same depth (~ 60 km). Hypocentral location of earthquakes within the overriding plate show that such a structure is active at 19°S [*Comte et al., 1999; David et al., 2002*] and 27°S [*Comte et al., 2002; Pardo et al., 2002*], and seismic images visualize a strong west-dipping reflector immediately above the slab at ~ 38°S [*Gross et al., 2007*].

If the intersection of the ramp with the slab is actually located everywhere at similar depths in the Chilean forearc, it is likely that this structure is controlled by processes directly related to the subduction factory. In fact, this intersection coincides with the deepest limit of the seismogenic contact along the Chilean subduction zone (i.e, along which thrust interplate earthquakes occur; *Suarez and Comte [1993]; Fig. 8*). In addition, the continental mantle in this zone presents sharp variations on  $V_p$  and  $V_p/V_s$  (**Fig. 5**), which are probably related to mantle serpentinization because the referred intersection also coincides with the 400°-500°C isotherm (**Fig. 6 and 8**), which is upper limit of serpentinite stability [*Carlson and Miller, 2003*].

(a) Immediately before basin inversion at ca. 22 Ma

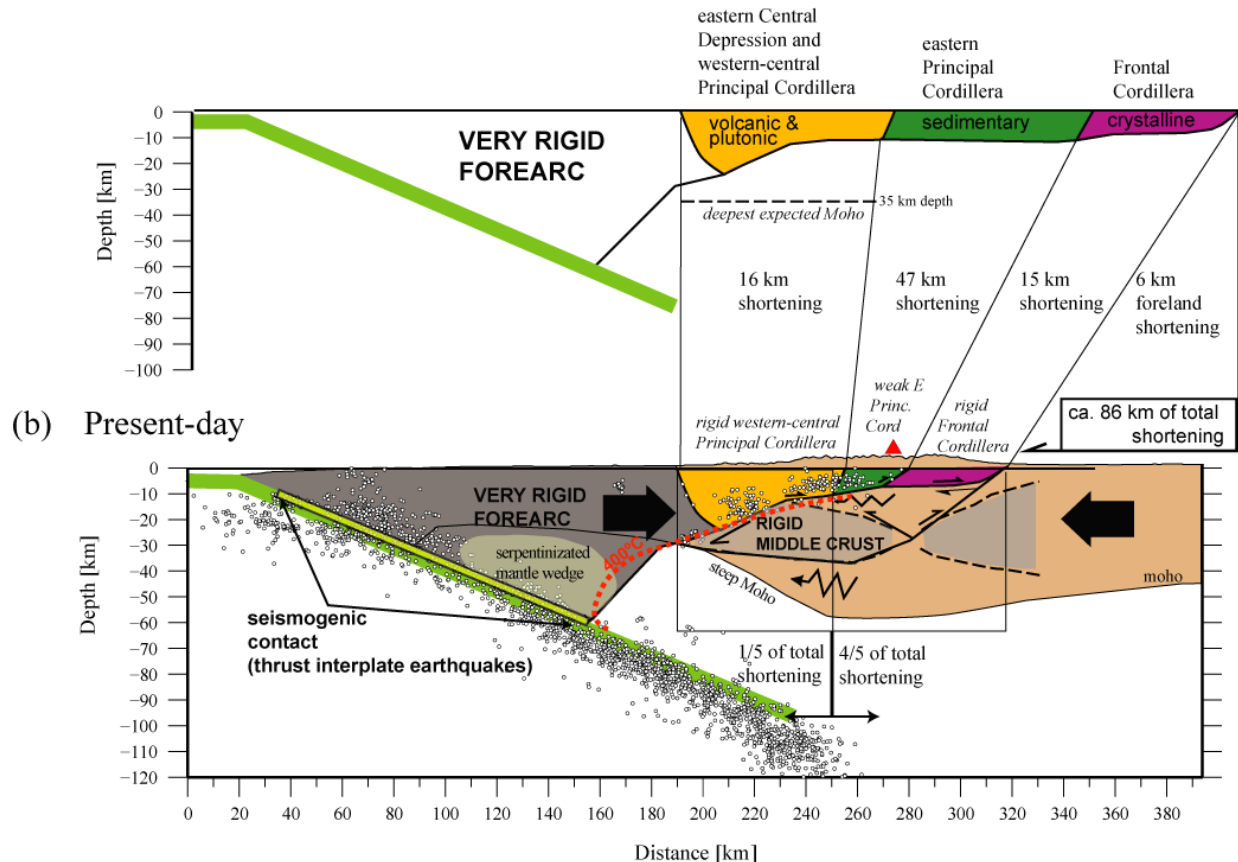


**Fig. 8.** Model for crustal growth and the relevance of the ramp-detachment structure at approximately 33°50'S. (a) Initial setting before shortening at 22 Ma. (b) Present-day crustal configuration. Shortening in the eastern Principal Cordillera, Frontal Cordillera, and foreland after *Giambiagi and Ramos [2002]*. Moho depth after *Tassara et al. [2006]*. 400°C isotherm based on *Oleskevich et al. [1999]* and *Yáñez and Cembrano [2004]*.

Empirical relationships between the degree of mantle serpentinization and  $V_p$  [*Carlson and Miller, 2003*] predict that the observed discontinuity would correspond to a change from ~0% to 20% of serpentinization at the conditions of pressure-temperature expected for that zone. In addition, the high  $V_p/V_s$  ratios observed at shallower depths than 60 km in the mantle wedge (**Fig. 5**) are also consistent with serpentinization (e.g., *Kamiya and Kobayashi [2000]*).

It is clear that an important shift on the mechanic behavior along the interplate contact occurs in the intersection of the ramp with the slab at nearly 60 km depth, which seems to be controlled by the thermal state. Following *Lamb and Davis [2003]* and *Lamb [2006]*, the stress produced by the plate convergence is mostly transferred to the overriding plate along the seismogenic interplate contact (**Fig. 8**). Likewise, *Tassara [2005]* proposed that the rigid behavior of the forearc (which is also strongly coupled with the slab) would promote more effectively the stress transfer to the continent. In this context, the ramp structure would not only control the strain transfer, but also delimitate upward the rocks that transmit part of the plate convergence forces toward the continental lithosphere, thus primarily controlling mountain building.

Based on the evidence presented in this work, the ramp-detachment structure seems to be the first-order feature controlling the transference of strain and stress from the subduction zone to the mountain belt not only in the Andes of Central Chile, but also probably along the entire Andean margin. Because this structure should be strongly controlled by the subduction factory processes, it is likely that the model presented in this work holds for other mountain belts formed in a subduction regime.

## **9. Conclusions**

Using the seismicity recorded in Central Chile by permanent and temporary networks, we performed a 3D tomography inversion that led to the relocalization of the most reliable hypocenters. We showed the presence of a crustal-scale ramp-flat structure that connects the subduction zone at  $\sim 60$  km depth with the mountain belt at  $\sim 10$  km. The flat segment crosses the entire mountain belt and correlates with the east-vergent detachment that accommodated most of the upper crustal shortening during the Neogene mountain building.

Geological cross-sections show that in the Chilean side of the belt, upper-crustal shortening was much smaller than in the Argentinean fold-and-thrust belts (1/5 versus 4/5 of the total shortening). In the western part of the Central Chile Andes, surface shortening does explain neither the present-day crustal thickness nor the uplift of this side of the mountain belt. In fact, most of the Neogene crustal thickening and uplift of the western part of the Central Chile Andes would result from the shortening accommodated beneath the detachment.

Despite huge latitudinal contrasts in the morphological and tectonic evolution of the Chilean Andes, a similar general lithospheric structural scheme in which a major east-vergent fault system emerges from the interplate contact area at  $\sim 60$  km depth and controls the structuration of the Andes has been proposed for Northern Chile. Inferences made on the south-central Chile region also suggest such a structure there. The intersection of the ramp with the slab coincides with the deepest limit of the seismogenic interplate contact. It is also marked by sharp variations in the overriding mantle seismic velocities that can be interpreted as a result of serpentinization of the lithospheric mantle wedge. Thus, we suggest that the subduction factory strongly controls the tectonic behavior of the forearc, producing the weak zones in which strain is transferred to the mountain range from the plate interface. The major east-vergent ramp delimitates upward rigid rocks that transmit part of the plate convergence forces toward the continental lithosphere.

This model suggests that the east-vergent ramp-flat structure is the first-order structure in the Andean mountain belt orogeny. Because this structural architecture is strongly controlled by the subduction factory, this model might be potentially applicable to other subduction margins. Hence, this architecture should be considered in models of the relationship between subduction processes and the overriding plate deformations.

## Acknowledgements

This work was funded by FONDECYT grant N° 1030965 and N°1070279, Bicentennial Program in Science and Technology grant ANILLO ACT N° 18, INSU grant “Relief de la Terre. Impact du climat sur la dynamique du relief des Andes: quantification et modélisation”, and a IRD doctoral grant to M. Farías. The authors particularly recognize the labor made by the Seismologic Survey at the University of Chile. We acknowledge Steven Roecker for providing the SPHREL90/SPHYFIT programs. Useful discussion with César Arriagada, Mario Pardo, Gérard Héral, Marcia Muñoz, Muriel Gerbault, Alejandra Reynaldos, and Gonzalo Yáñez helped develop and clarify our ideas. Some figures were made using GMT 4.1 [**Wessel and Smith, 1998**] and GRASS 6.2 (<http://grass.itc.it>) programs. GTOPO30 (<http://edcdaac.usgs.gov/gtopo30/gtopo30.html>), SRTM90 (<http://seamless.usgs.gov>) and the 2-minute gridded ocean bathymetry of **Smith and Sandwell [1997]** topographic and bathymetric data were used in some figures.

## References

- Abers, G.A., Roecker, S., 1991. Deep structure of an arc-continent collision: Earthquake relocation and inversion for upper mantle P and S wave velocities beneath Papua New Guinea. *J. Geophys. Res.* 96, 6379-6401.
- Allmendinger, R.W., Gubbels, T., 1996. Pure and simple shear plateau uplift, Altiplano-Puna, Argentina and Bolivia, *Tectonophysics* 259, 1-14.
- Barrientos, S., Vera, E., Alvarado, P., Monfret, T., 2004. Cristal seismicity in central Chile. *J. South Amer. Earth Sci.* 16, 759-768.
- Burov, E., Diament, M., 1995. The effective elastic thickness ( $T_e$ ) of continental lithosphere: what does it really mean? *J. Geophys. Res.* 107, 3905-3927.
- Burov, E., Diament, M., 1996. Isostasy, equivalent elastic thickness, and inelastic rheology of continents and oceans. *Geology* 24, 419-422.
- Carlson, R. L., Miller, D. J., 2003. Mantle wedge water contents estimated from seismic velocities in partially serpentinized peridotites. *Geophys. Res. Lett.* 30, 1250, doi:10.1029/2002GL016600.
- Carter, N.L., Tsenn, M.C., 1987. Flow properties of continental lithosphere. *Tectonophysics* 136, 27-63.
- Carter, W.D., Aguirre, L., 1965. Structural geology of the Aconcagua province and its relationship to the Central Valley Graben, Chile. *Geol. Soc. Amer. Bull.* 76, 651-664.
- Charrier, R., 1981. Geologie der chilenischen Hauptkordillere zwischen 34° und 34°30' südlicher Breite und ihre tektonische, magmatische und paläogeographische Entwicklung. *Berliner geowiss. Abh (A)* 36, 270pp.
- Charrier, R., Wyss, A.R., Flynn, J.J., Swisher, C.C., Norell, M.A., Zapatta, F., McKenna, C., Novacek, M.J., 1996. New evidence for late Mesozoic-early Cenozoic evolution of the Chilean Andes in the upper Tinguiririca valley (35°S), central Chile. *J. S. Am. Earth Sci.* 9, 393-422, doi:10.1016/S0895-9811(96)00035-1.
- Charrier, R., Baeza, O., Elgueta, S., Flynn, J.J., Gans, P., Kay, S.M., Muñoz, N., Wyss, A.R., Zurita, E., 2002. Evidence for Cenozoic extensional basin development and tectonic inversion south of the flat-slab segment, southern Central Andes, Chile (33°-36°S.L.). *J. S. Am. Earth Sci.* 15, 117-139, doi:10.1016/S0895-9811(02)00009-3.
- Charrier, R., Bustamante, M., Comte, D., Elgueta, S., Flynn, J.J., Iturra, N., Muñoz, N., Pardo, M., Thiele, R., Wyss, A.R., 2005. The Abanico Extensional Basin: Regional extension, chronology of tectonic inversion, and relation to shallow seismic activity and Andean uplift. *Neues Jahrb. Geol. P-A.* 236, 43-47.
- Cloetingh, S., Ziegler, P.A., Beekman, F., Andriessen, P.A.M., Hardebol, N., Dèzes, P., 2005. Intraplate deformation and 3D rheological structure of the Rhine Rift System and adjacent areas of the northern Alpine foreland, *Int. J. of Earth Sci.* 94, 758-778, doi:10.1007/s00531-005-0502-3.
- Comte, D., Dorbath, L., Pardo, M., Monfret, T., Haessler, H., Rivera, L., Frogneux, M., Glass, B., Meneses, C., 1999. A double-layered seismic zone in Arica, Northern Chile. *Geophys. Res. Lett.* 26, 1965-1968.
- Comte, D., Haessler, H., Dorbath, L., Pardo, M., Monfret, T., Lavenu, A., Pontoise, B., Hello, Y., 2002. Seismicity and stress distribution in the Copiapo, northern Chile subduction zone using combined on- and off-shore seismic observations. *Phys. Earth and Planet. In.* 132, 197-217.
- Cook, F.A., Varsek, J. L., 1994. Orogen-scale decollements. *Rev. Geophys.* 32, 37-60, doi:10.1029/93RG02515.
- Cristallini, E.O., Ramos, V.A., 2000. Thick-skinned and thin-skinned thrusting in La Ramada fold and thrust belt : Crustal evolution of the High Andes of San Juan, Argentina (32° SL). *Tectonophysics* 317, 205-235.

- Croft, D.A., Flynn, J.J., Wyss, A.R., 2003. Diversification of mesotheriids (Mammalia: Notoungulata: Typotheria) in the middle latitudes of South America. *Journal of Vertebrate Paleontology* 23, 43A.
- David, C., Martinod, J., Comte, D., Hérail, G., Haessler, H., 2002. Intracontinental seismicity and Neogene deformation of the Andean forearc in the region of Arica (18.5°S-19.5°S) (extended abstract). Proc. 5th International Symposium on Andean Geodynamics (ISAG), Toulouse, France.
- Davidson, J., Vicente, J.-C., 1973. Características paleogeográficas y estructurales del área fronteriza de las Nacientes del Teno (Chile) y Santa Elena (Argentina) (Cordillera Principal, 35° a 35°15' de latitud sur). In *Actas V Congreso Geológico Argentino Tomo V*, pp. 11-55.
- England, P., Molnar, P., 1991. Inferences of deviatoric stress in actively deforming belts from simple physical models. *Phil. Trans. R. Soc. Lond. A* 337, 151-164.
- Fariás, M., Comte, D., Charrier, R., 2006. Sismicidad superficial en Chile Central: Implicancias para el estado cortical y crecimiento de los Andes Central Australes (extended abstract). Proc. XI Congreso Geológico Chileno, Antofagasta, Chile.
- Fariás, M., Charrier, R., Comte, D., Martinod, J., Hérail, G., 2005. Late Cenozoic deformation and uplift of the western flank of the Altiplano: Evidence from the depositional, tectonic, and geomorphologic evolution and shallow seismic activity (northern Chile at 19°30'S). *Tectonics* 24, TC4001, doi:10.1029/2004TC001667.
- Flynn, J.J., Wyss, A.R., Charrier, R., Swisher, C.C., 1995. An Early Miocene anthropoid skull from the Chilean Andes. *Nature* 373, 603-607.
- Flynn, J.J., Wyss, A.R., Croft, D.A., Charrier, R., 2003. The Tinguiririca fauna, Chile: Biochronology, paleoecology, biogeography, and a new earliest Oligocene South American land mammal 'age'. *Palaeogeography, Palaeoclimatology, Palaeoecology* 195, 229-259.
- Fock, A., Charrier, R., Fariás, M., Muñoz, M., 2006. Fallas de vergencia oeste en la Cordillera Principal de Chile Central: Inversión de la cuenca de Abanico (33°-34°S). *Asociación Geológica Argentina, Serie: Publicación Especial* 6, 48-55.
- Fuentes, F., 2004. Petrología y metamorfismo de muy bajo grado de unidades volcánicas Oligoceno-Miocenas en la ladera occidental de los Andes de Chile Central (33°S). Ph.D. dissertation, Departamento de Geología Universidad de Chile, Santiago, Chile.
- García, M. 2002. Evolution Oligo-Miocéne de l'Altiplano Occidental (Arc et Avant-Arc du Nord Chili, Arica). Ph.D. Dissertation, Université Joseph Fourier, Grenoble, France.
- Giambiagi, L. B., Ramos, V. A., 2002. Structural evolution of the Andes between 33°30' and 33°45' S, above the transition zone between the flat and normal subduction segment, Argentina and Chile. *J. S. Am. Earth Sci.* 15, 99-114, doi:10.1016/S0895-9811(02)00008-1.
- Giambiagi, L.B., Ramos, V.A., Godoy, E., Alvarez, P.P., Orts, S., 2003. Cenozoic deformation and tectonic style of the Andes, between 33° and 34° south latitude. *Tectonics*, 22, 1041, doi:10.1029/2001TC001354.
- Godoy, E., Yáñez, G., Vera, E., 1999. Inversion of an Oligocene volcano-tectonic basin and uplift of its superimposed Miocene magmatic arc, Chilean central Andes: First seismic and gravity evidence. *Tectonophysics* 306, 217-326, doi:10.1016/S0040-1951(99)00046-3.
- Gripp, A.E., Gordon, R.G., 2002. Young tracks of hotspots and current plate velocities. *Geophys. J. Int.* 150, 321-361.
- Gross, K., Buske, S., Shapiro, S., Wigger, P., 2007. Seismic imaging of the subduction zone in southern central Chile (abstract). Proc. 20th Colloquium on Latin American Earth Science, Kiel, Germany.
- Gutscher, M.A., Maury, R., Eissen, J.P., Bourdon, E. 2000. Can slab melting be caused by flat subduction? *Geology* 28, 535-538.
- Hoke, G.D., Isacks, B.L., Jordan, T.E., Blanco, N., Tomlinson, A.J., Ramezani, J., in press. Geomorphic evidence for post-10 Ma uplift of the western flank of the Central Andes 18°30'-22°S. *Tectonics*, doi:10.1029/2006TC002082.
- Isacks, B.L., 1988. Uplift of the Central Andean Plateau and bending of the Bolivian Orocline. *J. Geophys. Res.* 93, 3211-3231.
- Kamiya, S., Kobayashi, Y., 2000. Seismological evidence for the existence of serpentinized wedge mantle. *Geophys. Res. Lett.* 27, 819-822
- Kay, S.M., Mpodozis, C., Ramos, V.A., Munizaga, F., 1991. Magma source variations for mid-late Tertiary magmatic rocks associated with a shallowing subduction zone and thickening crust in the central Andes. *Geol. Soc. Am. Special Paper* 265, 113-137.
- Kay, S.M., Godoy, E., Kurtz, A., 2005. Episodic arc migration, crustal thickening, subduction erosion, and magmatism in the south-central Andes. *Geol. Soc. Amer. Bull.* 117, 67-88.
- Klein, F.W., 1978. Hypocenter location program HYPOINVERSE. U.S. Geol. Surv., Open-File Rep. 78-694.
- Kono, M., Fukao, Y., Yamamoto, A., 1989. Mountain building in the Central Andes. *J. Geophys. Res.* 94, 3891-3905, doi:10.1029/88JB03954.

- Lamb, S., 2006. Shear stresses on megathrusts: Implications for mountain building behind subduction zones. *J. Geophys. Res.* 111, B07401, doi:10.1029/2005JB003916.
- Lamb, S., Davis, P., 2003. Cenozoic climate change as a possible cause for the rise of the Andes. *Nature* 425, 792-797.
- Lamb, S., Hoke, L., Kennan, L., Dewey, J., 1997. Cenozoic evolution of the central Andes in Bolivia and northern Chile. In: Burg, J.-P., and Ford, M. (Eds.), *Orogens through time*, Geol. Soc. Spec. Publ. 121, pp. 237-264.
- Legrand, D., Delouis, B., Dorbath, L., David, C., Campos, J., Marquéz, L., Thompson, J., Comte, D., 2007. Source parameters of the Mw=6.3 Aroma crustal earthquake of July 24, 2001 (northern Chile), and its aftershock sequence. *J. S. Am. Earth Sci.* 24, 58-68.
- Levi, B., Aguirre, L., Nyström, J., Padilla, H., Vergara, M., 1989. Low-grade regional metamorphism in the Mesozoic-Cenozoic volcanic sequences of the Central Chile. *Journal of Metamorphic Petrology* 7, 487-495.
- McClay, K.R., 1995. The geometries and kinematics of inverted fault systems: a review of analogue model studies. In Buchanan, P.G. (eds), *Basin Inversion*, Geological Society Special Publication 88, 97-118.
- McQuarrie, N., 2002. The kinematic history of the central Andean fold-thrust belt, Bolivia: implications for building a high plateau. *Geol. Soc. Amer. Bull.* 114, 950-963.
- Muñoz, N., Charrier, R., 1996. Uplift of the western border of the Altiplano on a west-vergent thrust system, northern Chile. *J. S. Am. Earth Sci.* 9, 171-181.
- Muñoz, M., Fuentes, F., Vergara, M., Aguirre, L., Nyström, J.O., Féraud, G., Demant, A., 2006. Abanico East Formation: Petrology and geochemistry of volcanic rocks venid the Cenozoic arc front in the Andean Cordillera, central Chile (33°50'S). *Rev. Geol. Chile* 33, 109-140.
- Nur, A., Ben-Avraham, Z., 1981. Volcanic gaps and the consumption of aseismic ridges in South America. *Mem. Geol. Soc. Amer.* 154, 729-740.
- Oleskevich, D.A., Hyndman, R.D., Wang, K., 1999. The updip and downdip limits to great subduction earthquakes: Thermal and structural models of Cascadia, south Alaska, SW Japan, and Chile. *J. Geophys. Res.*, 104, 14,965-14,992.
- Pardo, M., Comte, D., Monfret, T., 2002. Seismotectonic and stress distribution in the central Chile subduction zone. *J. S. Am. Earth Sci.* 15, 11-22, doi:10.1016/S0895-9811(02)00003-2.
- Pérez-Gussinyé, M., Lowry, A.R., Watts, A.B., 2007. Effective elastic thickness of South America and its implications for intracontinental deformation. *Geochem. Geophys. Geosyst.* 8, Q05009, doi:10.1029/2006GC001511.
- Pilger, R.H., 1981. Plate reconstruction, aseismic ridges, and low angle subduction beneath the Andes. *Geol. Soc. Amer. Bull.* 92, 448-456.
- Rauld R., Vargas, G., Armijo, R., Ormeño, A., Valderas, C., Campos, J., 2006. Cuantificación de escarpes de falla y deformación reciente en el frente cordillerano de Santiago (extended abstract). *Proc. XI Congreso Geológico Chileno*, Antofagasta, Chile.
- Riquelme, R., Hérail, G., Martinod, J., Charrier, R., Darrozes, J., 2007. Late Cenozoic geomorphologic signal of Andean forearc deformation and tilting associated with the uplift and climate changes of the Southern Atacama Desert (26°S-28°S). *Geomorphology* 86, 283-306, doi:10.1016/j.geomorph.2006.09.004.
- Roecker, S.W., Sabitova, T.M., Vinnik, L.P., Burmakov, Y.A., Golvanov, M.I., Mamatkanova, R., Munirova, L., 1993. Three-dimensional elastic wave velocity structure of the western and central Tien Shan. *J. Geophys. Res.* 98, 15779-15795.
- SEGEMAR, 1997. Mapa Geológico de la República Argentina escala 1:2 500 000. Servicio Geológico Minero Argentino, Buenos Aires, Argentina.
- SERNAGEOMIN, 2002. Mapa Geológico de Chile, escala 1:1 000 000. Map M61, Servicio Nacional de Geología y Minería, Santiago, Chile.
- Smith, W.H.F., Sandwell, D.T., 1997. Global sea floor topography from satellite altimetry and ship depth soundings. *Science* 277, 1956-1962.
- Suarez, G., Comte, D., 1993. Comment on "Seismic coupling along the Chilean subduction zone" by B.W. Ticherlaar and L.R. Ruff. *J. Geophys. Res.* 98, 15825-15828.
- Tassara, A., 2005. Interaction between the Nazca and South American plates and formation of the Altiplano-Puna plateau: Review of a flexural analysis along the Andean margin (15°-34°S). *Tectonophysics* 399, 39-57.
- Tassara, A., Götze, H.-J., Schmidt, S., Hackney, R., 2006. Three-dimensional density model of the Nazca plate and the Andean continental margin. *J. Geophys. Res.* 111, B09404, doi:10.1029/2005JB003976.
- Tassara, A., Swain, C., Hackney, R., Kirby, J., 2007. Elastic thickness of South America estimated using wavelets and satellite-derived gravity data. *Earth Planet. Sci. Lett.* 253, 17-36, doi:10.1016/j.epsl.2006.10.008.
- Thiele, R., 1980. Hoja Santiago, Región Metropolitana. Carta Geológica de Chile 39, Instituto de Investigaciones Geológicas, Santiago, Chile.
- Thierer, P.O., Flüh, E.R., Kopp, H., Tilmann, F., Comte, D., Contreras, S., 2005. Local earthquake monitoring offshore Valparaíso, Chile. *Neues Jahrb. Geol. P-A.*, 236, 173-183.

- Thomas, H., 1958. Geología de la Cordillera de la Costa entre el Valle de la Ligua y la Cuesta de Barriga. Boletín Instituto de Investigaciones Geológicas 2, Santiago.
- Uyeda, S., Kanamori, H., 1979. Back-arc opening and the mode of subduction. *J. Geophys. Res.* 84, 1049-1061.
- Vergara, M., Levi, B., Villarroel, R., 1993. Geothermal-type alteration in a butial metamorphosed volcanic pile, Central Chile. *Journal of Metamorphic Geology* 11, 449-454.
- Vergés, J., Ramos, V.A., Meigs, A., Cristallini, E., Bettini, F.H., Cortés, J.M., 2007. Crustal wedging triggering recent deformation in the Andean thrust front between 31°S and 33°S: Sierras Pampeanas-Precordillera interaction. *J. Geophys. Res.* 112, B03S15, doi:10.1029/2006JB004287.
- Victor, P., Oncken, O., Glodny, J., 2004. Uplift of the western Altiplano plateau: Evidence from the Precordillera between 20° and 21°S (northern Chile). *Tectonics* 23, TC4004, doi:10.1029/2003TC001519.
- Wessel, P., Smith, W.H.F., 1998. New, improved version of the Generic Mapping Tools released. *EOS Trans. AGU* 79, 579.
- Wyss, A.R., Norell, M.A., Flynn, J.J., Novacek, M.J., Charrier, R., McKenna, M.C., Frassinetti, D., Salinas, P., Meng, J., 1990. A new early Tertiary mammal fauna from central Chile: Implications for stratigraphy and tectonics. *Journal of Vertebrate Paleontology* 10, 518-522.
- Yáñez, G., Cembrano, J., 2004. Role of viscous plate coupling in the late Tertiary Andean tectonics. *J. Geophys. Res.* 109, B02407, doi:10.1029/2003JB002494.
- Yáñez, G., Ranero, C.R., von Huene, R., Díaz, J., 2001. Magnetic anomaly interpretation across the southern central Andes (32°-34°S): the role of the Juan Fernández Ridge in the late Tertiary evolution of the margin. *J. Geophys. Res.* 106, 6325-6345.